



## Adsorptive Removal of Cr(VI) and Cu(II) Ions from Water Solution using Graphene Oxide–Manganese Ferrite (GMF) Nanomaterials

S. Shahrin<sup>a,b</sup>, W. J. Lau<sup>\*a,b</sup>, P. S. Goh<sup>a,b</sup>, J. Jaafar<sup>a,b</sup>, A. F. Ismail<sup>a,b</sup>

<sup>a</sup> Advanced Membrane Technology Research Centre (AMTEC), Universiti Teknologi Malaysia, 81310 Skudai, Johor, Malaysia

<sup>b</sup> School of Chemical and Energy Engineering, Universiti Teknologi Malaysia, 81310 Skudai, Johor, Malaysia

### PAPER INFO

#### Paper history:

Received 19 December 2017

Received in revised form 21 March 2018

Accepted 21 March 2018

#### Keywords:

Nanomaterial  
Heavy Metals  
Adsorption  
Removal

### ABSTRACT

Chromium (Cr) and copper (Cu) are heavy metals known for their dangerous effect towards human health and could enter into human body mainly through ingestion. Over the years, different treatment methods have been used to eliminate heavy metal from raw water source and these include (co)precipitation, coagulation/flocculation, adsorption and ion-exchange. Nonetheless, adsorption is the most prominent method due to its high adsorption capacity and low cost. In this work, graphene oxide-manganese ferrite (GMF) nanomaterials were synthesized and used to remove Cr(VI) and Cu(II) ions from water solution based on adsorption mechanism. The synthesized nanomaterials were characterized using FTIR, BET and TEM prior to use in adsorption process. Batch adsorption studies were carried out to study the adsorption capacity and kinetic properties of the nanomaterials in eliminating two selective heavy metal ions. At optimum pH value, the maximum adsorption capacity for Cr(VI) and Cu(II) are 34.02 and 66.94 mg/g, respectively. The experimental data revealed that the adsorption isotherm best fitted Langmuir model and followed *Pseudo* second order.

doi: 10.5829/ije.2018.31.08b.24

### NOMENCLATURE

Q	Adsorption efficiency	1/n	Freundlich exponent
C <sub>i</sub>	Initial concentration, (mg/L)	q <sub>e</sub>	Adsorption capacity at equilibrium (mg/g)
C <sub>f</sub>	Final concentration, (mg/L)	q <sub>m</sub>	Maximum adsorption capacity (mg/g)
q	Adsorption capacity (mg/g)	t	Time (min)
C <sub>e</sub>	Equilibrium concentration	q <sub>t</sub>	adsorption capacity at time t, (mg/g)
K	Langmuir constant	K <sub>1</sub>	Pseudo first order constant, (L/min)
K <sub>F</sub>	Empirical Freundlich constant	K <sub>2</sub>	Pseudo second order constant, (g/mg.min)

## 1. INTRODUCTION

Worldwide urbanization and industrialization have caused severe contamination of heavy metal in water sources. Heavy metals such as arsenic, lead, mercury, chromium and copper is considered as serious threat towards environment and human health due to their toxicity, mobility and fatality [1-4]. Chromium (Cr(VI)) and copper (Cu(II)) are among the heavy metals that can cause lung cancer and cellular damage with long term exposure. Both heavy metals exist in two oxidation state, i.e., Cr(VI), Cr(III) [5], Cu(I) and Cu(II) [2].

Cr(VI) is 500 times more fatal than Cr(III) due to its toxicity [6]. The transition between Cu(II) and Cu(I) can result in generation of superoxide radicals [2]. In view of this, United States Environmental Protection Agency (USEPA) has set the maximum level of total chromium and copper in standard drinking water at 100 ppb and 1300 ppb, respectively.

Cr(VI) and Cu(II) remediation have captured the attention from both academia and industry worldwide. Of the various treatment methods, adsorption is the most promising one as it is cost effective and can be used to eliminate not only heavy metals but also other contaminants [6, 7]. Various types of adsorbents have been used for heavy metal removal. These include metal

\*Corresponding Author Email: lwoeijye@utm.my (W. J. Lau)

oxide, mixed metal oxide, clays, activated carbon, etc. Mixed metal oxide such as manganese ferrite promised high adsorption capacity towards heavy metal removal [8]. Nonetheless, this nanoparticle tends to agglomerate easily due to its strong dipole-dipole interactions, which affect magnetic properties and sedimentation [9]. Graphene oxide (GO), on the other hand, has demonstrated good properties such as low density, high surface area and large number of oxygenated functional group that will enhance adsorption capacity [8, 10]. Decorating manganese ferrite onto GO surface is a promising solution to handle the sedimentation, agglomeration and dispersion problems of manganese ferrite.

The objective of this study is to synthesize new type of hybrid material, i.e., graphene oxide–manganese ferrite (GMF) using chemical co-precipitation for adsorptive removal of Cr(VI) and Cu(II) ions. The nanomaterial was characterized by Fourier transform Infrared (FTIR), X-ray diffraction (XRD), Brunauer, Emmet and Teller (BET) and transmission electron microscope (TEM). The application of nanomaterial for both Cr(VI) and Cu(II) ions removal was investigated via batch adsorption study by varying parameters such as pH, ion concentration and contact time. Isotherm and kinetic models, i.e., Freundlich, Langmuir, Pseudo first and second order models were used to determine the nanomaterial adsorption mechanism.

## 2. MATERIALS

Iron (III) chloride hexahydrate ( $\text{FeCl}_3 \cdot 6\text{H}_2\text{O}$ , 98%, Sigma Aldrich), manganese (II) sulphate monohydrate ( $\text{MnSO}_4 \cdot \text{H}_2\text{O}$ ,  $\geq 99\%$ , Sigma Aldrich) and sodium hydroxide pallet ( $\text{NaOH}$ , 99%, Merck) was used to synthesize GMF. Graphite powder ( $< 20\mu\text{m}$ , Sigma Aldrich) used to synthesize GO, later used to prepare GMF hybrid. Sulphuric acid ( $\text{H}_2\text{SO}_4$ , 95-97%, Merck), sodium nitrate ( $\text{NaNO}_3$ , Riedel-de Haen), potassium permanganate ( $\text{KMnO}_4$ ,  $> 99\%$ , Sigma Aldrich) and hydrogen peroxide 30% ( $\text{H}_2\text{O}_2$ , Merck) were used to oxidize graphite to GO. Barium chloride 2-hydrate ( $\text{BaCl}_2 \cdot 2\text{H}_2\text{O}$ , Riedel-de Haen) and hydrochloric acid ( $\text{HCl}$ , 37%, Merck) were used during GO washing process. Millipore RO water (ASTM Type III) was used for nanomaterial washing and stock solution preparation. Acetone (RCI Labscan) was used for final nanomaterial washing

## 3. METHOD

### 3. 1. Preparation of Graphene Oxide–Manganese Ferrite hybrids

Firstly, GO was prepared using Hummers' method [9, 11] where in brief graphite was oxidized by  $\text{KMnO}_4$  in acidic condition at temperature

below  $5^\circ\text{C}$ . Afterwards, GMF was prepared by chemical co-precipitation method as previously described by Kumar Nair [8]. GO (0.5g) was dispersed in RO (400 mL) water followed by 5-min ultrasonication. Then,  $\text{FeCl}_3 \cdot 6\text{H}_2\text{O}$  (2.7g) and  $\text{MnSO}_4 \cdot \text{H}_2\text{O}$  (0.845g) were added into the resulting solution and stirred for 30 min. While stirring, temperature of the suspension was raised and maintained at  $80^\circ\text{C}$ . The pH was adjusted to 10.5 using 8 M  $\text{NaOH}$  solution and let to stir for another 5 min, then cooled to room temperature. Blackish precipitated product was then washed until neutral with RO water and acetone for further purification. Finally, the resulting suspension was filtered followed by drying at  $60^\circ\text{C}$  for 24 h.

**3. 2. Adsorption Study** Batch adsorption study was carried out in order to determine the GMF adsorption and kinetic behaviour towards heavy metal removal. GMF adsorption behaviour was studied by varying pH values of Cr(VI) and Cu(II) solution in order to determine the optimum pH condition. Initial pH value was varied in range of 2-10 using either 1 N  $\text{HCl}$  or 1 M  $\text{NaOH}$  solution. In separate experiment, adsorption isotherm of GMF (dosage: 1 g/L) was investigated at optimum pH condition with different initial ion concentration in range of 5-200 mg/L. Cr(VI) and Cu(II) solution were freshly prepared from 1000mg/L stock solution. All mixtures were shaken using digital orbital shaker (Intertek, Heathrow Scientific) at 250 rpm for 48 h. Afterwards, GMF was separated from Cr(VI) and Cu(II) solution by filtration using  $0.45\mu\text{m}$  polytetrafluoroethylene (PTFE) syringe filter. For kinetic studies, pH value was fixed at 2 and 4.5 for Cr(VI) and Cu(II), respectively with initial concentration of 100 mg/L and adsorption time of 5-2880 min. Cr(VI) and Cu(II) final concentration was measured by flame atomic absorption spectrometer (AA-7000, Shimadzu). All measurements were taken in duplicate and average values of two measurements were recorded.

**3. 3. Characterization** FTIR for GMF was measured in wavelength range of  $400\text{--}4000\text{ cm}^{-1}$  using Spectrum One FTIR Spectrometer (Perkin Elmer). GMF surface area was measured via BET method by 3Flex by  $\text{N}_2$  gas adsorption at 77 K. TEM was used to identify GMF morphology structure.

## 4. RESULTS AND DISCUSSION

**4. 1. Nanomaterial Characterization** Adsorption FTIR peaks of both GO and GMF in Figure 1 show similar pattern at  $1711\text{ cm}^{-1}$ ,  $1623\text{ cm}^{-1}$ ,  $1375\text{ cm}^{-1}$ ,  $1242\text{ cm}^{-1}$  and  $1056\text{ cm}^{-1}$ . These peaks are attributed to C=O stretching from  $\text{--COOH}$  group, C=C stretching due to water molecule adsorbed, deformation of  $\text{--OH}$ , C–O

stretching from alkoxy group, C—O—C stretching form from epoxy group, respectively. Additional peaks at 492  $\text{cm}^{-1}$  and 607  $\text{cm}^{-1}$  in the GMF are due to metal-O stretching that represents vibrations of manganese ferrite [10-12]. The results confirm that GMF was successfully synthesized.

The result from BET analysis shows that the surface area of GO and GMF are 441.03 and 105.41  $\text{m}^2/\text{g}$ , respectively. The surface area of GMF is reduced when manganese ferrite is incorporated into the GO nanosheet, indicating that part of the GO pores are filled or occupied by manganese ferrite particles [13]. Figure 2 shows the morphology of nanomaterials observed by TEM. As can be seen, the synthesized GO is packed and rippled and exhibits flake-like structure. The GMF meanwhile is found to have spherical and rod-like particles distributed on the surface of GO nanosheet. This confirms the presence of manganese ferrite in the GMF. Similar observation was also reported in other work [9, 12-15].

**4. 2. Adsorption Study** The performance of GMF towards Cr(VI) and Cu(II) adsorption was studied by varying pH, initial concentration and contact time. The adsorption efficiency (Q) was calculated using Equation (1).

$$Q (\%) = \frac{C_i - C_f}{C_f} \times 100 \quad (1)$$

where  $C_i$  is the initial concentration (mg/L) and  $C_f$  is the final concentration (mg/L).

**4. 2. 1. pH Effect** Operational pH condition in the adsorption study is crucial as it affects the adsorption capacity by altering nanomaterial solubility and heavy metal ions dissociation [3]. Figure 3 shows the dependencies of Cr(VI) and Cu(II) ion adsorption efficiency towards GMF at different pHs. Notably, the optimum pH for Cr(VI) and Cu(II) are at pH 2 (40%) and pH 4 (38%), respectively. Adsorption efficiency for Cr(VI) ion decreases as the pH value increases.

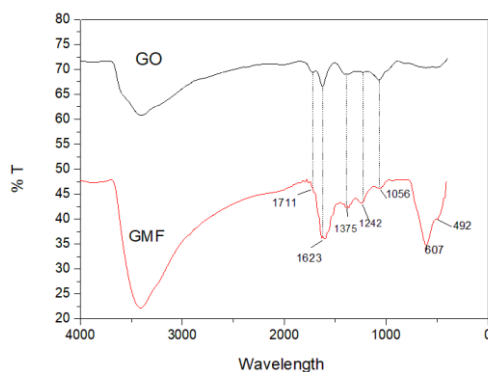


Figure 1. FTIR spectra of GO and GMF

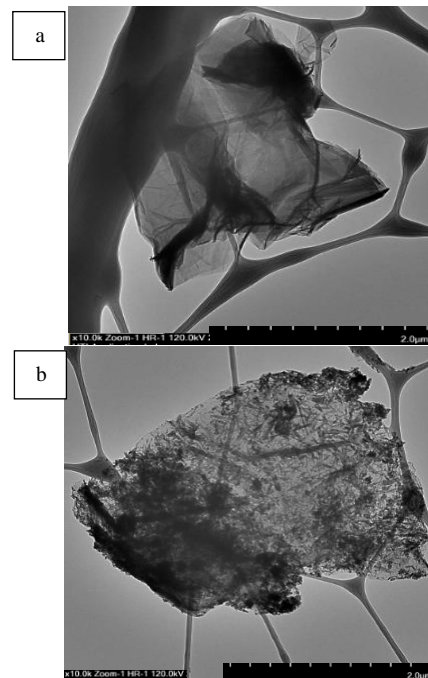


Figure 2. TEM image of (a) GO and (b) GMF

While for Cu(II) ion, it is found that the efficiency reduces at pH 2, increases at pH 4 and decreases with increasing pH after pH 4. This adsorption pattern can be explained by the separation of GMF, Cr(VI) and Cu(II) ions, that form differently depending on the pH condition. At pH 2, hexavalent chromium exists in  $\text{HCrO}_4^-$  and  $\text{CrO}_7^{2-}$  ion differs from copper which exists in  $\text{Cu}^{2+}$  ion. Nonetheless, copper will exist in form of  $\text{Cu}(\text{OH})_3^-$  and  $\text{Cu}(\text{OH})_4^{2-}$  ion at pH above 4 [13, 15, 16]. While, at low pH concentration, GMF is positively charged ( $-\text{OH}_2^+$ ) [10]. This explains the optimum adsorption efficiency for Cr(VI) and Cu(II) ion is due to electrostatic attraction between GMF and heavy metal ion at pH 2 and 4, respectively. Meanwhile, the observation at pH 2 by Cu(II) ions is attributed to ionic repulsion between  $\text{Cu}^{2+}$  and  $\text{H}^+$  ions.

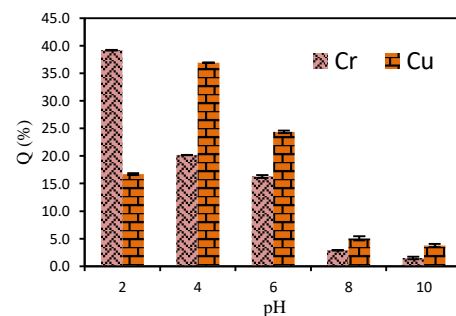


Figure 3. The dependencies of Cr(VI) and Cu(II) ion adsorption towards different pH values with initial concentration of 50 mg/L

**4. 2. 2. Adsorption Isotherm** The adsorption isotherm of Cr(VI) and Cu(II) ion was studied by varying its initial concentration in the range of 5-300 mg/L at its respective optimum pH condition. As shown in Figure 4, the adsorption capacity increases with increasing initial concentration until it achieves plateau. The maximum adsorption capacity for Cr(VI) and Cu(II) ion are reported to be 34.02 and 66.94 mg/g, respectively. To further understand the adsorption isotherm mechanism, the data were plotted in linear form using Equations 2 (Langmuir Isotherm) and 3 (Freundlich Isotherm), respectively.

$$\frac{C_e}{q} = \frac{1}{Kq_m} + \frac{C_e}{q_m} \tag{2}$$

$$\text{Log } q_e = \frac{\text{Log } K_F + 1}{n \text{ Log } C_e} \tag{3}$$

where  $q$  is adsorption capacity,  $C_e$  is equilibrium concentration (mg/L),  $K$  is Langmuir constant,  $K_F$  is empirical Freundlich constant,  $1/n$  is Freundlich exponent and  $q_e$  is adsorption capacity at equilibrium (mg/g), and  $q_m$  is maximum adsorption capacity (mg/g). Notably, adsorption data were well fitted with Langmuir adsorption that suggest the Cr(VI) and Cu(II) adsorption occurred at homogenous surface by monolayer adsorption.

**4. 2. 3. Adsorption Kinetic** Adsorptions kinetic was studied by varying the contact time between nanomaterial and heavy metals ion. As illustrated in Figure 5a, the adsorption capacity increases with contact time until it achieved plateau at 1440 and 2880 min, respectively. To further investigate the rate of metal uptake by time, experimental data were plotted using linear equation of pseudo first and second order as expressed in Equations (4) and (5), respectively.

$$\text{Log } (q_e - q_t) = \frac{\text{Log}(q_e) - k_1}{2.303t} \tag{4}$$

$$\frac{t}{q_t} = \frac{1}{K_2 q_e^2} + \frac{1}{q_e} t \tag{5}$$

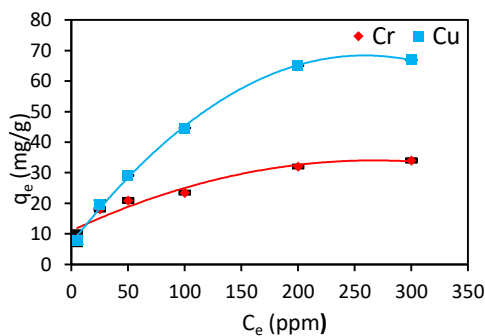


**Figure 4.** Langmuir adsorption isotherm for Cr(VI) and Cu(II) at different initial concentration under optimum pH condition (pH 2 for Cr(VI) and pH 4 for Cu(II))

where,  $q_e$  is adsorption capacity at equilibrium (mg/g),  $q_t$  is adsorption capacity at time  $t$  (min),  $k_1$  (L/min) and  $k_2$  (g/mg.min) is the rate constant of pseudo first and second order. Notably, the experimental data were best fitted with pseudo second order model as the correlation coefficient,  $R^2$  value was very near to 1, so as the value of expected  $q_e$  and experimental  $q_e$  was in close agreement (see Table 1). This suggests that Cr(VI) and Cu(II) adsorption towards GMF is based on chemisorption.

**4. 2. 4. Adsorption Mechanism** The adsorption mechanism of Cr(VI) and Cu(II) towards GMF can be further discussed as follows. The speciation of metal ion and GMF is dependent on the solution pH. Oxygenated groups presented in the GO nanosheet and metal oxide could act as active sites to absorb Cr(VI) and Cu(II) ions via electrostatic attraction mechanism [17-19].

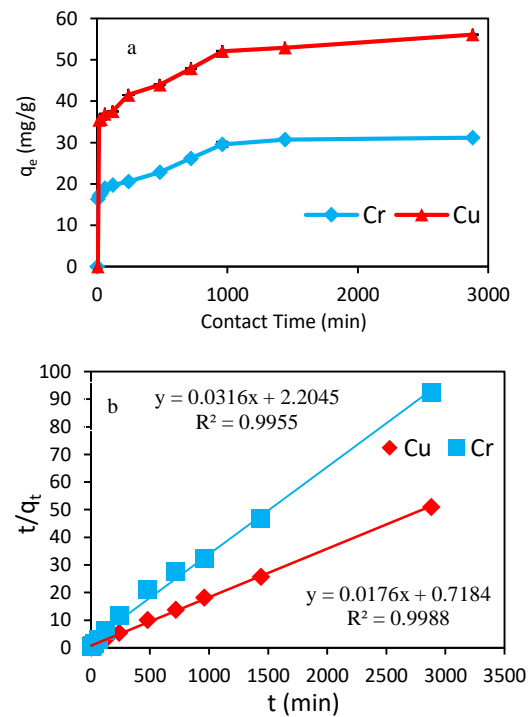
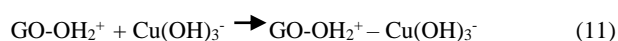


**Figure 5.** Adsorption kinetic graph, (a) Effect of contact time of towards Cr(VI) and Cu(II) adsorption with 1.0 g/L GMF at initial concentration of 100 mg/L (pH value was kept at 2 and 4 for Cr(VI) and Cu(II), respectively) and (b) Pseudo-second order kinetic of Cr(VI) and Cu(II) ions onto the GMF

**TABLE 1.** Experimental and expected  $q_e$  value by Pseudo second order kinetic model for Cr(VI) and Cu(II) ion

Heavy metal	Experimental $q_e$ (mg/g)	Expected $q_e$ (mg/g)
Cr(VI)	31.75	31.64
Cu(II)	56.48	56.81

This mechanism is most likely occurred at pH 2 and 4, respectively. In the acidic condition, the -OH group in the GO and metal oxide is positively charged and converted to  $-\text{OH}_2^+$  [10]. Meanwhile, Cr(VI) and Cu(II) are in the form of  $\text{HCrO}_4^-/\text{CrO}_7^{2-}$  ion and  $\text{Cu}(\text{OH})_3^-/\text{Cu}(\text{OH})_4^{2-}$ , respectively [13, 15, 16]. Hence,  $-\text{OH}_2^+$  in GMF will attract  $\text{HCrO}_4^-/\text{CrO}_7^{2-}$  and  $\text{Cu}(\text{OH})_3^-/\text{Cu}(\text{OH})_4^{2-}$  ion by electrostatic attraction and form complex ion, causing high adsorption capacity. The adsorption reactions are shown in the following equations.



## 5. CONCLUSION

In this study, adsorption of GMF nanomaterials towards Cr(VI) and Cu(II) ions was studied by varying the pH, initial concentration and contact time during adsorption process. The synthesized GMF was characterized by FTIR, BET and TEM. It was found that the optimum pH condition for Cr(VI) and Cu(II) adsorption rate was at pH 2 and 4, respectively. It was also found that all data were best fitted with Langmuir adsorption model, suggesting the adsorption occurred at homogenous surface by monolayer adsorption, with maximum adsorption capacity of Cr(VI) and Cu(II) at 34.02 and 66.94 mg/g, respectively. Effect of contact time indicated that the adsorption process followed pseudo second order, where the adsorption of Cr(VI) and Cu(II) involved chemisorption process. High adsorption capacity of GMF towards Cr(VI) and Cu(II) ions indicated that the potential of this nanomaterial for treating water sources containing selective heavy metal ions.

## 6. REFERENCES

1. Maleki, A., Hayati, B., Naghizadeh, M. and Joo, S.W., "Adsorption of hexavalent chromium by metal organic frameworks from aqueous solution", *Journal of Industrial and Engineering Chemistry*, Vol. 28, (2015), 211-216.
2. Reddi, M.G., Gomathi, T., Saranya, M. and Sudha, P., "Adsorption and kinetic studies on the removal of chromium and copper onto chitosan-g-malic anhydride-g-ethylene dimethacrylate", *International Journal of Biological Macromolecules*, Vol. 104, (2017), 1578-1585.
3. Meng, Y., Chen, D., Sun, Y., Jiao, D., Zeng, D. and Liu, Z., "Adsorption of  $\text{Cu}^{2+}$  ions using chitosan-modified magnetic Mn ferrite nanoparticles synthesized by microwave-assisted hydrothermal method", *Applied Surface Science*, Vol. 324, (2015), 745-750.
4. Khashij, M., Mousavi, S., Mehralian, M. and Massoudinejad, M., "Removal of  $\text{Fe}^{2+}$  from aqueous solution using manganese oxide coated zeolite and iron oxide coated zeolite", *International Journal of Engineering-Transactions B: Applications*, Vol. 29, No. 11, (2016), 1587.
5. Karimi, M., Shojaei, A., Nematollahzadeh, A. and Abdekhodaie, M.J., "Column study of Cr(VI) adsorption onto modified silica-polyacrylamide microspheres composite", *Chemical Engineering Journal*, Vol. 210, (2012), 280-288.
6. Samani, M.R., Borghei, S.M., Olad, A. and Chaichi, M.J., "Removal of chromium from aqueous solution using polyaniline-poly ethylene glycol composite", *Journal of Hazardous Materials*, Vol. 184, No. 1-3, (2010), 248-254.
7. Fu, D., He, Z., Su, S., Xu, B., Liu, Y. and Zhao, Y., "Fabrication of  $\alpha$ -FeOOH decorated graphene oxide-carbon nanotubes aerogel and its application in adsorption of arsenic species", *Journal of Colloid and Interface Science*, Vol. 505, (2017), 105-114.
8. Kumar, S., Nair, R.R., Pillai, P.B., Gupta, S.N., Iyengar, M. and Sood, A., "Graphene oxide-mnfe<sub>2</sub>o<sub>4</sub> magnetic nanohybrids for efficient removal of lead and arsenic from water", *ACS Applied Materials & Interfaces*, Vol. 6, No. 20, (2014), 17426-17436.
9. Wang, G., Ma, Y., Tong, Y. and Dong, X., "Development of manganese ferrite/graphene oxide nanocomposites for magnetorheological fluid with enhanced sedimentation stability", *Journal of Industrial and Engineering Chemistry*, Vol. 48, (2017), 142-150.
10. Sarker, M., Song, J.Y. and Jhung, S.H., "Adsorption of organic arsenic acids from water over functionalized metal-organic frameworks", *Journal of Hazardous Materials*, Vol. 335, (2017), 162-169.
11. Hummers Jr, W.S. and Offeman, R.E., "Preparation of graphitic oxide", *Journal of the American Chemical Society*, Vol. 80, No. 6, (1958), 1339-1339.
12. Lai, G., Lau, W., Goh, P., Ismail, A., Yusof, N. and Tan, Y., "Graphene oxide incorporated thin film nanocomposite nanofiltration membrane for enhanced salt removal performance", *Desalination*, Vol. 387, (2016), 14-24.
13. Reddy, D.H.K. and Yun, Y.-S., "Spinel ferrite magnetic adsorbents: Alternative future materials for water purification", *Coordination Chemistry Reviews*, Vol. 315, (2016), 90-111.
14. Guo, P., Zhang, G., Yu, J., Li, H. and Zhao, X., "Controlled synthesis, magnetic and photocatalytic properties of hollow spheres and colloidal nanocrystal clusters of manganese ferrite", *Colloids and Surfaces A: Physicochemical and Engineering Aspects*, Vol. 395, (2012), 168-174.
15. Badii, E., Sangpour, P., Bagheri, M. and Pazouki, M., "Graphene oxide antibacterial sheets: Synthesis and characterization (research note)", *International Journal of Engineering-Transactions C: Aspects*, Vol. 27, No. 12, (2014), 1803-1808.
16. Liu, Y., Chen, M. and Yongmei, H., "Study on the adsorption of Cu(II) by EDTA functionalized Fe<sub>3</sub>O<sub>4</sub> magnetic nanoparticles", *Chemical Engineering Journal*, Vol. 218, (2013), 46-54.
17. Harijan, D.K. and Chandra, V., "Polyaniline functionalized graphene sheets for treatment of toxic hexavalent chromium", *Journal of Environmental Chemical Engineering*, Vol. 4, No. 3, (2016), 3006-3012.

18. Lv, X., Zhang, Y., Fu, W., Cao, J., Zhang, J., Ma, H. and Jiang, G., "Zero-valent iron nanoparticles embedded into reduced graphene oxide-alginate beads for efficient chromium (vi) removal", *Journal of Colloid and Interface Science*, Vol. 506, (2017), 633-643.
19. Zavareh, S., Behrouzi, Z. and Avanes, A., "Cu (ii) binded chitosan/fe<sub>3</sub>o<sub>4</sub> nanocomposite as a new biosorbent for efficient and selective removal of phosphate", *International Journal of Biological Macromolecules*, Vol. 101, (2017), 40-50.

## Adsorptive Removal of Cr(VI) and Cu(II) Ions from Water Solution using Graphene Oxide–Manganese Ferrite (GMF) Nanomaterials

S. Shahrin<sup>a,b</sup>, W. J. Lau<sup>a,b</sup>, P. S. Goh<sup>a,b</sup>, J. Jaafar<sup>a,b</sup>, A. F. Ismail<sup>a,b</sup>

<sup>a</sup> Advanced Membrane Technology Research Centre (AMTEC), Universiti Teknologi Malaysia, 81310 Skudai, Johor, Malaysia

<sup>b</sup> School of Chemical and Energy Engineering, Universiti Teknologi Malaysia, Johor, 81310 Skudai, Johor, Malaysia

### P A P E R I N F O

چکیده

#### Paper history:

Received 19 December 2017

Received in revised form 21 March 2018

Accepted 21 March 2018

#### Keywords:

Nanomaterial  
Heavy Metals  
Adsorption  
Removal

کروم و مس (*Cu*) فلزات سنگین هستند که به خاطر تأثیرات خطرناک آنها نسبت به سلامت انسان شناخته شده است و می‌توانند به طور عمده از طریق خوراک وارد بدن انسان شوند. در طول سالها، روش های مختلف درمان برای حذف فلز سنگین از منبع آب خام مورد استفاده قرار گرفته است و شامل بارش (co)، انعقاد / *flocculation* جذب و تبادل یونی است. با این حال، جذب به عنوان یکی از مهم ترین روش ها به دلیل ظرفیت جذب بالا و هزینه کم است. در این کار، نانومواد فریت اکسید منگنز گرافین (GMF) گرافین سنتز شده و برای حذف یونهای *Cr (VI)* و *Cu (II)* از محلول آب بر اساس مکانیزم جذب استفاده می‌شود. نانو مواد سنتز شده با استفاده از *BET*، *FTIR* و *TEM* قبل از استفاده در فرایند جذب مشخص شد. مطالعات جذب دسته ای برای بررسی ظرفیت جذب و خواص جنبشی نانومواد در حذف دو یون فلز انتخابی سنگین انجام شده است. در *pH* مطلوب، حداکثر ظرفیت جذب *Cr (VI)* و *Cu (II)* به ترتیب 34.02 و 94.66 میلی گرم بر گرم است. داده های آزمایشی نشان داد که ایزوترم جذب به بهترین وجه مدل لانگمویر و به ترتیب پسیو دوم را دنبال می‌کند.

doi: 10.5829/ije.2018.31.08b.24